QUARTERLY OF APPLIED MATHEMATICS
VOLUME LXXIII, NUMBER 1
MARCH 2015, PAGES 177–199
S 0033-569X(2015)01377-0
Article electronically published on January 22, 2015

RUN-UP AMPLIFICATION OF TRANSIENT LONG WAVES

By

THEMISTOKLIS S. STEFANAKIS (*CMLA, ENS Cachan, CNRS, 61 Avenue du Président Wilson, F-94230 Cachan, France – and – UCD School of Mathematical Sciences, University College Dublin, Belfield, Dublin 4, Ireland*),

SHANSHAN XU (*UCD School of Mathematical Sciences, University College Dublin, Belfield, Dublin 4, Ireland*),

DENYS DUTYKH (*UCD School of Mathematical Sciences, University College Dublin, Belfield, Dublin 4, Ireland – and – Université de Savoie-CNRS Laboratoire de Mathématiques LAMA - UMR, 5127 Campus Scientifique, 73376 Le Bourget-du-Lac, France*),

AND

FRÉDÉRIC DIAS (*UCD School of Mathematical Sciences, University College Dublin, Belfield, Dublin 4, Ireland – and – CMLA, ENS Cachan, CNRS, 61 Avenue du Président Wilson, F-94230 Cachan, France*)

Abstract. The extreme characteristics of the run-up of transient long waves are studied in this paper. First, we give a brief overview of the existing theory which is mainly based on the hodograph transformation (Carrier and Greenspan (1958)). Then, using numerical simulations, we build on the work of Stefanakis et al. (2011) for an infinite sloping beach and we find that resonant run-up amplification of monochromatic waves is robust to spectral perturbations of the incoming wave and that resonant regimes do exist for certain values of the frequency. In the canonical problem of a finite beach attached to a constant depth region, resonance can only be observed when the incoming wavelength is larger than the distance from the undisturbed shoreline to the seaward boundary. Wavefront steepness is also found to affect wave run-up, with steeper waves reaching higher run-up values.

1. Introduction. Long wave run-up, the maximum elevation of wave uprush on a beach above still water level, is difficult to observe in nature in real time due to the large physical dimensions of the phenomenon and to the catastrophic consequences it

Received May 13, 2013.
2010 *Mathematics Subject Classification.* Primary 76B15, 35Q35.
E-mail address: stefanakis.themistoklis@gmail.com
E-mail address: shanshan.xu@ucdconnect.ie
E-mail address: Denys.Dutykh@univ.savoie.fr
E-mail address: frederic.dias@ucd.ie

sometimes leads to, the most physical manifestation of a long wave being a tsunami. Tidal waves, meteotsunamis [3] and storm surges are also long waves.

Most observational data concerning run-up are collected during post-tsunami surveys [4]. Nevertheless, this data does not offer any information, by itself, on the time history of the event, which leads field scientists to rely on interviews with eye-witnesses, who, in some cases, have reported that it is not always the first wave which results in the worst damage. Moreover, unexpected extreme localized run-up values have been measured during several tsunami events, such as in Java 1994 [5], Java 2006 [6], Chile 2010 [7] and Japan 2011 [8]. Hence, a question arises whether these extreme run-up values are related to non-leading waves.

Stefanakis et al. [2] showed that for a given plane beach slope there exist wave frequencies that lead to resonant long wave run-up amplification by non-leading waves. These results were confirmed in wave tank physical experiments by Ezersky et al. [9], who distinguished the frequency that leads to resonant run-up from the resonant frequency of the wavemaker. They also observed a secondary resonant regime which had not been identified before. They recognized that the resonant state occurs when the Bessel function $J_0(\sqrt{4\omega^2 L/g\tan\theta}) = 0$, as predicted by the linear theory [10], where ω is the angular frequency of the wave, $\tan\theta$ is the beach slope, L is the horizontal distance from the undisturbed shoreline to the point where the wave amplitude is imposed and g is the acceleration due to gravity. Several other possible explanations for the observed extreme run-up values are also available.

Miles [11] described the conditions for harbor resonance and the importance of the Helmholtz mode to tsunami response, and later Kajiura [12] introduced the notion of bay resonance. Agnon and Mei [13] and Grataloup and Mei [14] studied the long wave resonance due to wave trapping and wave-wave interactions. Munk et al. [15] and Rabinovich and Leviant [16] studied wave resonance in the context of shelf resonance, which occurs when tidal waves have a wavelength four times larger than the continental shelf width. Fritz et al. [6] suggested that the extreme run-up values measured after the Java 2006 tsunami could be explained by a submarine landslide triggered by the earthquake. All of the above underline the critical role of bathymetry and coastal geometry to long wave propagation and run-up. In a recent study, Kanoglu et al. [17] argued that finite-crest length effects may produce focusing. Nonetheless, resonant run-up has already been documented for the case of short waves [18] with an interesting description:

> [Resonant run-up] occurs when run-down is in a low position and wave breaking takes place simultaneously and repeatedly close to that location.

Similar observations have been made by Stefanakis et al. [2].

On a theoretical basis, the main mathematical difficulty of the run-up problem is the moving shoreline. Progress was made through the introduction of the Carrier and Greenspan (CG) transformation [1], which leads to the reduction of the two Nonlinear Shallow Water Equations (NSWE) into one linear, but the ingenuity of this transformation is that in the transformed space the moving shoreline is static. With the aid of the CG transformation several significant contributions have been made to this long wave run-up problem [19–25].

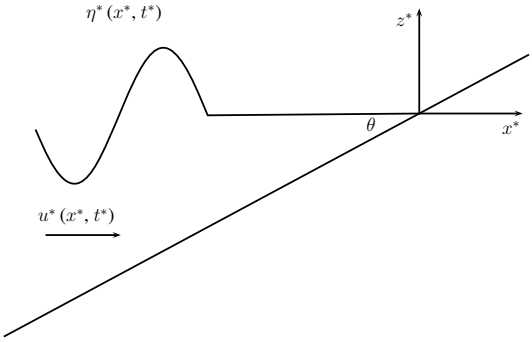

FIG. 1. Geometry of the problem of the run-up of transient long waves along a sloping beach.

A thorough review with additional results on its relation to the surf-similarity is given by Madsen and Fuhrman [26]. These theoretical results do not exhibit any resonant regimes and were reproduced numerically by Madsen and Fuhrman [27] by placing a relaxation zone close to the wave generation region, which absorbs the reflected wavefield. These sponge layers are widely used because the combination of incoming and outgoing waves at the boundary still remains poorly understood. These are artifacts and are not part of the governing wave equations.

In the present paper, we first provide an overview of the theory behind long wave run-up on an infinite plane beach,[1] and we confirm the resonance results of Stefanakis et al. [2] with more geophysically relevant bottom slopes. We also prove their robustness to modal perturbations. The case of a piecewise linear beach is described next where we show both analytically and computationally the existence of resonant states. Then, we explore whether resonance can be observed when a sloping beach is connected to a constant depth region, and we test the effect of wave nonlinearity and how the results relate to the theory. Finally, we discuss the effect the boundary condition has on the resonant run-up amplification.

2. Statement of problem and method of analytical solution. Here we present a review of the analytical solution. Consider a wave propagation problem described by the one-dimensional NSWE

$$\frac{\partial \eta^*}{\partial t^*} + \frac{\partial}{\partial x^*}\left[(h+\eta^*)\,u^*\right] = 0, \quad \frac{\partial u^*}{\partial t^*} + u^*\frac{\partial u^*}{\partial x^*} + g\frac{\partial \eta^*}{\partial x^*} = 0, \tag{1}$$

where $z^* = \eta^*(x^*, t^*)$ is the free surface elevation, $h(x^*)$ is the water depth, $u^*(x^*, t^*)$ is the depth-averaged horizontal velocity and g is the acceleration due to gravity. Consider a topography consisting of a sloping beach with unperturbed water depth varying linearly with the horizontal coordinate $h(x^*) = -\alpha x^*$, where $\alpha = \tan\theta$ is the bottom slope (see Figure 1).

[1]Since the theory has been developed over the last five decades, it is useful to provide a short review of the major advances in a condensed form. That way, the alternative approach proposed in the present paper will appear more clear.

In order to solve equations (1), appropriate initial and boundary conditions must be supplied. In most wave problems, one must provide the initial conditions $\eta^*(x^*,0)$ and $u^*(x^*,0)$ (for tsunamis, it is usually assumed that $u^*(x^*,0)=0$). The boundary condition far from the tsunami source area ("left boundary") is

$$\eta^*(x^*,t^*)\to 0,\quad u^*(x^*,t^*)\to 0\quad (x^*\to-\infty). \tag{2}$$

If the tsunami source is far from the shore, it is convenient not to include the source area in the fluid domain, and then apply the following "left" (incoming wave) boundary condition at some point $x^*=x_0^*$:

$$u^*(x_0^*,t)=\sqrt{g/h(x_0^*)}\eta^*(x_0^*,t), \tag{3}$$

which corresponds to the tsunami wave approaching the shore. Another boundary condition is boundedness on the unknown moving boundary,

$$h(x^*)+\eta^*(x^*,t^*)=0\,, \tag{4}$$

which determines the location of the moving shoreline. This condition (4) is the main difference from the classical formulations of the Cauchy problem for hyperbolic systems.

There is an analytical method for solving this system, based on the use of the Riemann invariants. These invariants for a plane beach are

$$I_\pm=u^*\pm 2\sqrt{g(-\alpha x^*+\eta^*)}+g\alpha t^*, \tag{5}$$

and the system (1) can be rewritten as

$$\frac{\partial I_\pm}{\partial t^*}+\left(\frac{3}{4}I_\pm+\frac{1}{4}I_\mp-g\alpha t^*\right)\frac{\partial I_\pm}{\partial x^*}=0. \tag{6}$$

It is important to mention that this approach is applied for water waves on a beach of constant slope, and there are no rigorous results for arbitrary depth profiles $h(x^*)$. The existence of Riemann invariants in the general case is an open mathematical problem.

The hodograph transformation can then be applied to the system (6), assuming that the determinant of the Jacobian $J=\partial(x^*,t^*)/\partial(I_+,I_-)$ does not vanish. This determinant vanishes when the wave breaks; we note that Synolakis [21] has argued that this point is simply where the hodograph transformation becomes singular and the interpretation is that the wave breaks, and in fact corresponds to breaking during the rundown, at least for solitary waves. As a result, the following set of equations is derived:

$$\frac{\partial x^*}{\partial I_\mp}-\left(\frac{3}{4}I_\pm+\frac{1}{4}I_\mp-g\alpha t^*\right)\frac{\partial t^*}{\partial I_\mp}=0. \tag{7}$$

These equations are nonlinear, but they can be reduced to a linear equation by eliminating $x^*(I_+,I_-)$:

$$\frac{\partial^2 t^*}{\partial I_+\,\partial I_-}+\frac{3}{2(I_+-I_-)}\left(\frac{\partial t^*}{\partial I_-}-\frac{\partial t^*}{\partial I_+}\right)=0. \tag{8}$$

It is convenient to introduce the new variables,

$$\lambda=\frac{1}{2}(I_++I_-)=u^*+g\alpha t^*,\quad \sigma=\frac{1}{2}(I_+-I_-)=2\sqrt{g(-\alpha x^*+\eta^*)}. \tag{9}$$

Then the system (8) takes the form

$$\sigma \left(\frac{\partial^2 t^*}{\partial \lambda^2} - \frac{\partial^2 t^*}{\partial \sigma^2} \right) - 3 \frac{\partial t^*}{\partial \sigma} = 0. \tag{10}$$

Expressing the time t^* from (9),

$$t^* = \frac{\lambda - u^*}{g\alpha}, \tag{11}$$

and substituting

$$u^* = \frac{1}{\sigma} \frac{\partial \Phi}{\partial \sigma}, \tag{12}$$

we finally rewrite (10) in the form of the classical cylindrical wave equation,

$$\frac{\partial^2 \Phi}{\partial \lambda^2} - \frac{\partial^2 \Phi}{\partial \sigma^2} - \frac{1}{\sigma} \frac{\partial \Phi}{\partial \sigma} = 0. \tag{13}$$

All physical variables can be expressed through the function $\Phi(\sigma, \lambda)$. In addition to the time t^* (11) and the velocity u^* (12), the horizontal coordinate x^* and the water displacement η^* are given by

$$x^* = \frac{1}{2g\alpha} \left(\frac{\partial \Phi}{\partial \lambda} - u^{*2} - \frac{\sigma^2}{2} \right), \tag{14}$$

$$\eta^* = \frac{1}{2g} \left(\frac{\partial \Phi}{\partial \lambda} - u^{*2} \right). \tag{15}$$

Therefore, the initial set of nonlinear shallow water equations has been reduced to the linear wave equation (13) and all physical variables can be found via Φ using simple operations. The main advantage of this form of the nonlinear shallow water system is that the moving shoreline corresponds to $\sigma = 0$ (since the total depth $h(x^*)+\eta^*(x^*, t^*) = 0$) and therefore (13) is solved in the half-space $0 \le \sigma < \infty$ with a fixed boundary, unlike the initial equations. The linear cylindrical wave equation (13) is well-known in mathematical physics, and its solution can be presented in various forms such as Green's function, Hankel and Fourier transforms. Using its solution, the wave field in "physical" variables can be found from algebraic manipulations. Detailed analyses of the wave transformation and run-up have been performed for various initial conditions; see for instance [24, 28, 29].

Meanwhile, the typical situation in tsunamis is that the wave approaches the shore from deep water, where the wave can be considered as linear. In this case it is possible to find the function Φ without using the implicit formulas of the hodograph transformation. Let us consider the linear version of the shallow water system:

$$\frac{\partial u^*}{\partial t^*} + g \frac{\partial \eta^*}{\partial x^*} = 0, \quad \frac{\partial \eta^*}{\partial t^*} + \frac{\partial}{\partial x^*} \left(-\alpha x^* u^* \right) = 0, \tag{16}$$

and apply the linearized version of the hodograph transformation

$$\eta^* = \frac{1}{2g} \frac{\partial \Phi_l}{\partial \lambda_l}, \quad u^* = \frac{1}{\sigma_l} \frac{\partial \Phi_l}{\partial \sigma_l}, \quad x^* = -\frac{\sigma_l^2}{4g\alpha}, \quad t^* = \frac{\lambda_l}{g\alpha}, \tag{17}$$

where the subscript l denotes quantities derived from linear theory. In this case the system (16) reduces naturally to the same linear cylindrical wave equation

$$\frac{\partial^2 \Phi_l}{\partial \lambda_l^2} - \frac{\partial^2 \Phi_l}{\partial \sigma_l^2} - \frac{1}{\sigma_l}\frac{\partial \Phi_l}{\partial \sigma_l} = 0, \tag{18}$$

which has the same form as in nonlinear theory (13). If the initial conditions for the wave field are determined far from the shoreline where the wave is linear, then the initial conditions for both equations (13) and (18) are the same, and therefore, their solutions will be the same,

$$\Phi(\sigma, \lambda) = \Phi_l(\sigma_l, \lambda_l), \tag{19}$$

after replacing the arguments. So the function Φ can be found from linear theory.

From the operational point of view, it is important to know the extreme run-up characteristics like run-up height, run-down amplitude, onshore and offshore velocity; these characteristics can be calculated within the framework of linear theory. This surprising result, also noted by Synolakis [21, 30], can be explained as follows. Indeed, it follows from (19) that extreme values of Φ and its derivatives are the same. But for a moving shoreline ($\sigma = 0$) in extreme points of run-up or run-down, the velocity is zero, and the expressions of the hodograph transformations (15) and (17) coincide. So, it is believed that the extreme characteristics of tsunami run-up which determine the flooding zone can be found from linear theory despite the real nonlinear character of the wave process in the nearshore area, and this is an important result for tsunami engineering.

Moreover, the nonlinear dynamics of the moving shoreline ($\sigma = 0$) can be easily derived using linear theory. It follows from (11) that the moving shoreline velocity is

$$u^*(\lambda, \sigma = 0) = \lambda - g\alpha t^*, \tag{20}$$

or in equivalent form

$$u^*(t^*) = u_l^*(t^* + u^*/g\alpha), \tag{21}$$

where the function $u_l^*(\lambda)$ is found from Φ. Therefore, it can be found from linear theory (it is the velocity at the point $x^* = 0$). Similarly, the water displacement should be found first from linear theory (at the point $x^* = 0$),

$$z_l^*(t^*) = \eta_l^*(x^* = 0, t^*) = \alpha \int u_l^*(t^*) dt^*, \tag{22}$$

and then one can find the "real" nonlinear vertical displacement of the moving shoreline,

$$z^*(t^*) = \eta^*(\sigma = 0) = \alpha \int u^*(t^*) dt^* = z_l^*(t^* + u^*/\alpha g) - u^{*2}(t^*)/2g. \tag{23}$$

As can be seen from these formulas, the extreme values of functions in linear and nonlinear theories coincide, as was pointed out already. The manifestation of nonlinearity is in the shape of the water oscillations on shore due to the nonlinear transformation (21).

As an example, let us consider the run-up of monochromatic waves on an infinite beach. It is enough to consider first the linear problem in the framework of the cylindrical wave equation (18). The elementary bounded solution is

$$\eta^*(x^*, t^*) = \eta_R J_0\left(\sqrt{\frac{4\omega^2 |x^*|}{g\alpha}}\right) \cos \omega t^*, \tag{24}$$

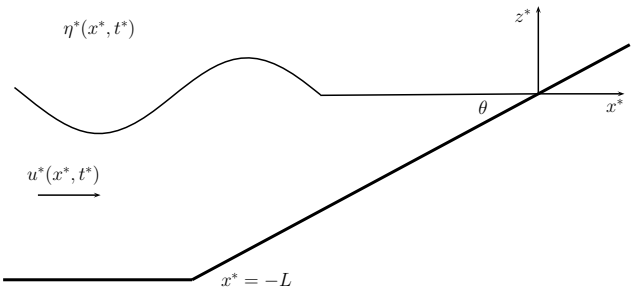

FIG. 2. The geometry of a plane beach connected to a region of constant depth.

with η_R an arbitrary constant. Using asymptotic expressions for the Bessel function J_0 around zero and matching with the solution of the mild slope equation (see [26]), one finds that the wave field far from the shoreline consists of the linear superposition of two waves propagating in opposite directions and having the same amplitudes (a standing wave):

$$\eta^*(x^*,t^*) = 2\eta_0 \left(\frac{L}{|x^*|}\right)^{1/4} \cos\left(2\omega\sqrt{\frac{|x^*|}{g\alpha}} + \varphi\right)\cos\omega t^*, \tag{25}$$

where the incident wave amplitude has been fixed to η_0 at the coordinate $x^* = -L$. The coefficient of wave amplification in the run-up stage is found as

$$\frac{\eta_R}{\eta_0} = 2\left(\frac{\pi^2\omega^2 L}{g\alpha}\right)^{1/4} = 2\pi\sqrt{\frac{2L}{\lambda_0}}, \tag{26}$$

where $\lambda_0 = 2\pi\sqrt{g\alpha L}/\omega$ is the wavelength of the incident wave.

3. A more realistic example. The rigorous theory described above is valid for waves in a wedge of constant slope. For all other depth profiles rigorous analytical results are absent. Real bathymetries, which are complex in the ocean, can be approximated by a beach of constant slope in the vicinity of the shore only. If the "matching" point is relatively far from the shoreline, the linear theory can be applied for waves in a basin of complex bathymetry except in the nearshore area. Within this approximation, and arguing as in [21], the 1D linear wave equation

$$\frac{\partial^2\eta^*}{\partial t^{*2}} - \frac{\partial}{\partial x^*}\left(c^2(x^*)\frac{\partial\eta^*}{\partial x^*}\right) = 0, \quad c^2(x^*) = gh(x^*) \tag{27}$$

should be solved analytically or numerically, and then its solution should be matched with the rigorous solution of the run-up problem described above. The canonical topography is presented in Figure 2, which is often realized in laboratory experiments [21]. The elementary solution of the wave equation (27) for a basin of constant depth h_0 is the superposition of incident and reflected waves

$$\eta^*(x^*,t^*) = \eta_0\exp[i\omega(t^* - x^*/c)] + A_r\exp[i\omega(t^* + x^*/c)] + \text{c.c.}, \quad c = \sqrt{gh_0} \tag{28}$$

with η_0 real and A_r complex, and this solution should be matched with (24) at the point $x^* = -L$ using the continuity of $\eta^*(x^*)$ and $d\eta^*/dx^*$. As a result, the unknown constants

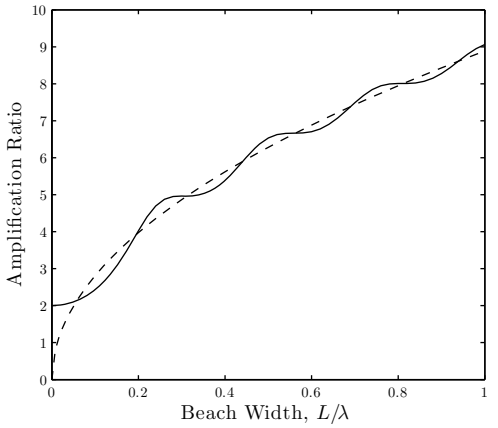

FIG. 3. Run-up height of a sine wave arriving from a basin of constant depth. The solid line is formula (29) and the dashed line is the result for an infinite beach of constant slope (26).

A_r and η_R can be calculated from the boundary conditions at $x^* = -L$, and the run-up amplitude is

$$\frac{\eta_R}{\eta_0} = \frac{2}{\sqrt{J_0^2(\chi) + J_1^2(\chi)}}, \quad \chi = \frac{2\omega L}{c} = 4\pi \frac{L}{\lambda_0}. \tag{29}$$

This is displayed in Figure 3. The solid line is formula (29) and the dashed line is the previous result for a beach of constant slope (26). One can see that the agreement between both curves is quite good.

4. Numerical results. The solutions described in the previous section are standing waves. If the motion starts at $t = 0$, i.e. it is not a steady state motion, one does not have a standing wave at the beginning. A standing wave requires time to develop, and during that time, run-up amplification can be significant if the left boundary is a physical node in the developed standing wave solution. In their monograph [31], Billingham and King suppose that at $x^* = -L$ there is an incident wave $\eta^*(-L, t^*) = 2\eta_0 \cos \omega t^*$. Matching the solution (24) with it at $x^* = -L$ yields

$$\eta^*(x^*, t^*) = 2\eta_0 J_0 \left(\sqrt{\frac{4\omega^2 |x^*|}{g\alpha}} \right) / J_0 \left(\sqrt{\frac{4\omega^2 L}{g\alpha}} \right) \cos \omega t^*. \tag{30}$$

There is indeed the possibility of a resonance, which occurs when $2\omega\sqrt{L/g\alpha}$ is a zero of J_0 and the solution (30) is then unbounded. Another way to look at this resonance is to consider Figure 9(a) in [26]. Resonance occurs when ones tries to force the wave amplitude to a finite value at one of the nodes of the solution (24). We will describe below how this resonance can occur in numerical as well as laboratory experiments.

4.1. *Waves on a plane beach.* We present some additional results on the resonant long wave run-up phenomenon on a plane beach described by Stefanakis et al. [2]. Namely, we look at the maximum run-up amplification of monochromatic waves, but this time we use milder slopes, which are more geophysically relevant ($\tan\theta = 0.02\,;\, 0.05\,;\, 0.1$). For

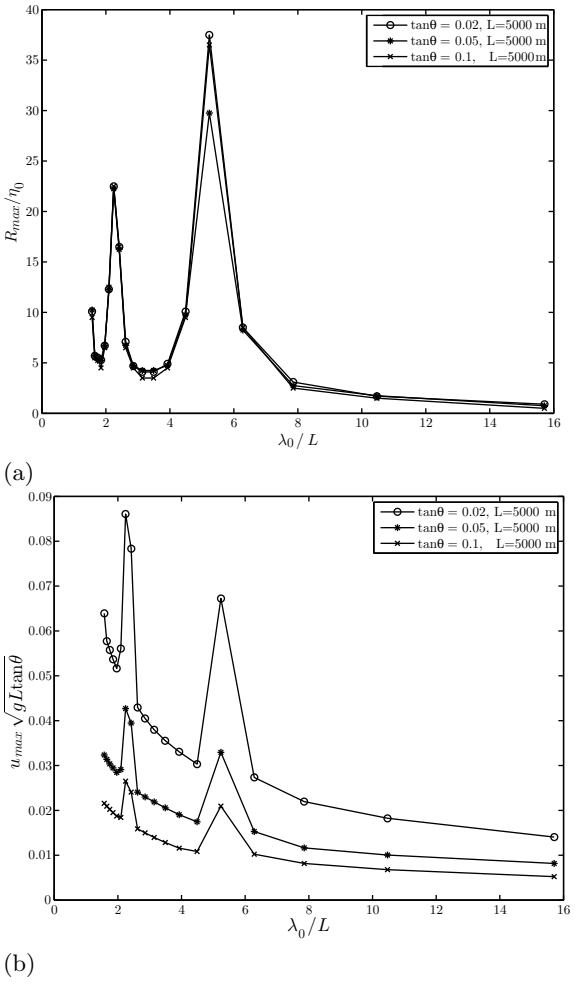

FIG. 4. Maximum run-up amplification $R_{\max}/\eta_0$ (a) and maximum horizontal velocity amplification (b) of monochromatic waves on a plane beach with respect to nondimensional wavelength for three different slopes, namely $\tan\theta = 0.02\,;\, 0.05\,;\, 0.1$ ($L = 5000$ m). Resonance is observed when the incoming wavelength is approximately 2.4 and 5.2 times the beach length.

our simulations, we used the NSWE in one dimension, which were solved numerically by a Finite Volume Characteristic Flux scheme with UNO2 reconstruction for higher order terms, and a third order Runge-Kutta time discretization. The left boundary condition is implemented as in [32]. This model was described in detail and validated by Dutykh et al. [33]. Monochromatic forcing ($\eta^*(-L, t^*) = 2\eta_0 \cos\omega t^*$) on an infinite sloping beach was found to lead to resonant run-up by non-leading waves (Figure 4a) when the nondimensional wavelength is $\lambda_0/L \approx 5.2$, where $\lambda_0 = 2\pi\sqrt{g\alpha L}/\omega$ is the incident wavelength, which comes as a direct consequence of (30) when the wave at the seaward boundary is specified, since resonant states can be identified with the roots of the Bessel

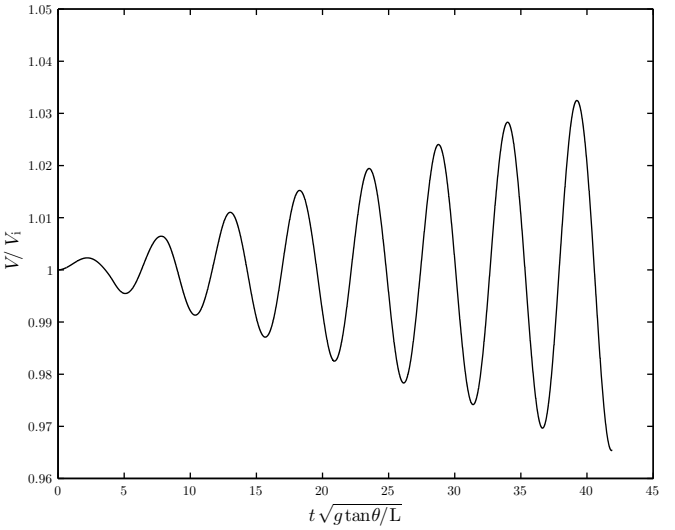

FIG. 5. Evolution of the volume of fluid V inside the computational domain during resonance ($\alpha = 0.02$, $L = 5000$ m, $\lambda_0/L = 5.2$). V_i is the initial volume.

function J_0. Resonance is also observed for the maximum horizontal velocities assumed by the waves (Figure 4b) which are found at the shoreline. Since

$$\eta^*(x^*, t^*) = \eta_R J_0(\sigma) \cos \omega t^* \ , \ u^*(x^*, t^*) = -\frac{2\omega\eta_R}{\sigma \tan\theta} J_1(\sigma) \sin \omega t^* \tag{31}$$

where

$$\sigma = 2\omega \sqrt{\frac{|x^*|}{g \tan\theta}} \tag{32}$$

and

$$\lim_{\sigma \to 0} \frac{J_1(\sigma)}{\sigma} = \frac{1}{2}, \tag{33}$$

then the shoreline velocity is

$$u_s^*(t^*) = -\frac{\omega\eta_R}{\tan\theta} \sin \omega t^*, \tag{34}$$

which implies that when the run-up is resonant, so is the shoreline velocity. The resonance mechanism was found to rely on a synchronization between incident and receding waves, but should be distinguished from wavemaker resonance since the computational domain is not closed (Figure 5), as it would be in a laboratory setting, and we can observe strong inflow-outflow during run-up and run-down. Furthermore, the experiments of Ezersky et al. [9] confirmed this claim by observing that the resonant frequency of the system is different from the frequency that leads to the resonant run-up.

The spatio-temporal behavior of the nondimensional horizontal velocity is shown in Figure 6. For visualization purposes, we plot only the last 500 m of the beach to the left of the initial shoreline position. We can observe that in the resonant regime, after the run-down induced by the leading wave, during run-up of subsequent waves, a fixed spatial point undergoes an abrupt change of velocity, from highly negative to highly

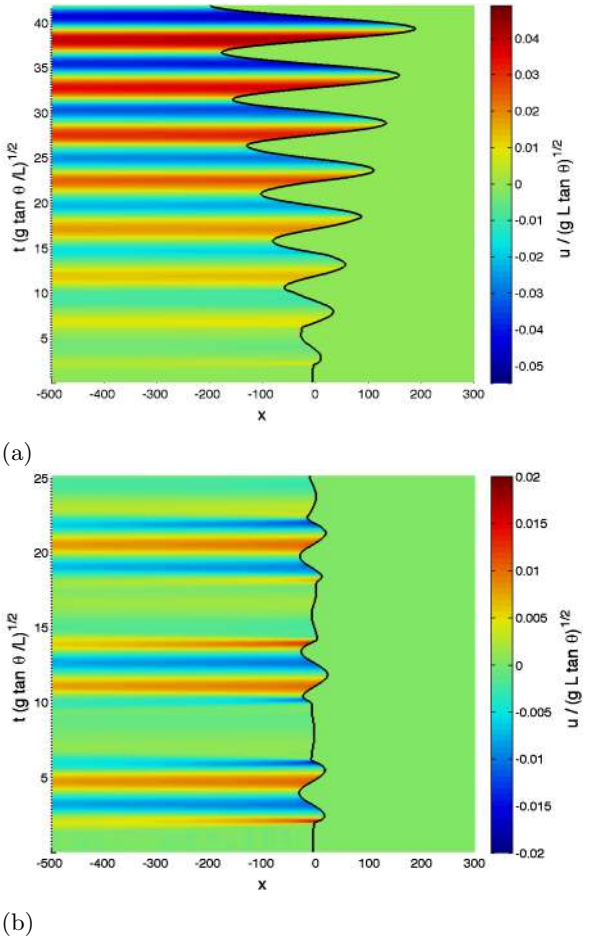

FIG. 6. Spatio-temporal behaviour of nondimensional horizontal velocity $u/(g\tan\theta L)^{1/2}$ in the resonant regime (a) and nonresonant regime (b). The black line describes the evolution of the shoreline position in time. In both cases $\tan\theta = 0.05$ and $L = 5000$ m.

positive values. Furthermore, the maximum absolute velocity increases over time in the resonant regime, while this is not true in the nonresonant case. To give a feeling of dimensions, imagine a plane beach with $\tan\theta = 0.01$ and an incoming wave of amplitude $\eta_0 = 1$ m at $L = 10,000$ m offshore where the water depth is $h_0 = 100$ m. For that wave to be in the resonant regime, its wavelength has to be approximately $52,000$ m. If there is a run-up amplification close to 40, this means that $\max u_s \approx 15$ m/s according to (34).

In order to increase our confidence in the numerical solver that we use, we ran simulations using VOLNA [34], an NSWE solver in two horizontal dimensions. VOLNA has been validated with the Catalina benchmark problems [35], established by the National Oceanic and Atmospheric Administration (NOAA) Center for Tsunami Research. They

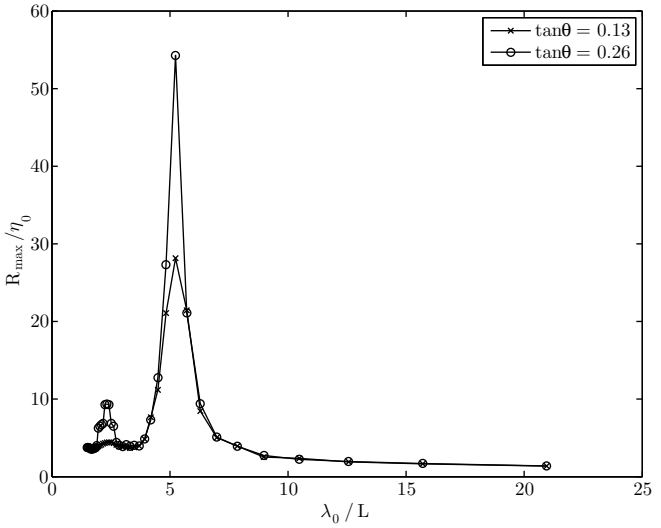

FIG. 7. Maximum run-up of monochromatic waves on a plane beach as a function of nondimensional wavelength for two different slopes, $\tan\theta = 0.13$ and 0.26 ($L = 12.5$ m). The results were obtained with VOLNA.

consist of a series of test cases based on analytical, experimental and field observations. We tested the maximum run-up on plane beaches with slopes $\tan\theta = 0.13; 0.26$ when the beach length is $L = 12.5$ m. We used a smaller beach length in order to limit the computational cost of the 2D simulations, and chose to follow the same setup as [2]. The results (Figure 7) are in good agreement with the results obtained before (Figure 2 in [2]), and the same resonant regime is observed again. Consequently, due to the confidence in the results we obtained and the reduced computational cost, we continued with the NSWE solver in one horizontal dimension.

In order to further investigate the effects of modal interactions in the resonant regime, we tested incoming waves of bichromatic modal structure. To remain consistent with the monochromatic case, each mode had half the amplitude of the equivalent monochromatic wave (η_0). Our computations (Figure 8) show that no important new interactions occur. When one of the two frequencies is resonant, the run-up is dominated by it, while the other does not alter the dynamics. If both frequencies are resonant, their constructive interference is small overall and does not differ significantly from the equivalent monochromatic resonant state. Therefore, this result indicates that the resonant run-up mechanism is robust and is not restricted to monochromatic waves only.

To investigate the robustness of the resonant run-up mechanism, we introduced ten semi-random perturbation components to the monochromatic wave signal. The amplitude of the perturbations followed a normal distribution with zero mean and standard deviation much less than the wave amplitude η_0. The perturbation frequency followed the lognormal distribution. The monochromatic wave and a corresponding semi-randomly perturbed signal in physical and Fourier spaces are shown in Figure 9. By running the simulation in the resonant regime when the slope $\alpha = 0.02$ and $L = 5000$ m, we obtained

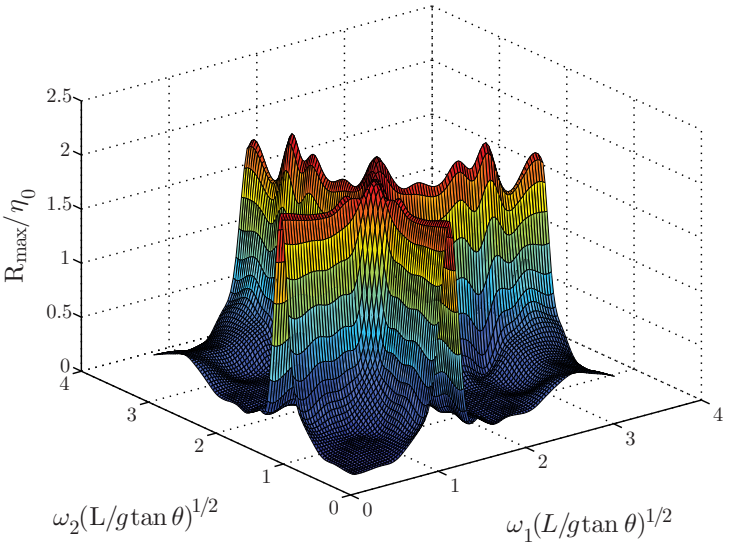

FIG. 8. Maximum run-up of bichromatic waves with respect to nondimensional frequency ($\tan\theta = 0.13$, $L = 12.5$ m).

the same run-up timeseries that we would otherwise have obtained with the unperturbed monochromatic wave (Figure 10). Therefore, we can conclude that the resonant run-up mechanism is robust and the resonant frequency dominates the run-up.

4.2. *Piecewise linear bathymetry.* Kanoglu and Synolakis [36] developed a general methodology to study the problem of long wave run-up over a piecewise linear bathymetry and applied it to the study of solitary wave run-up, but in their formulation, the last offshore segment of the bathymetry consisted of a flat bottom. Here we will only use two uniformly sloping regions, as in Figure 11. Following Lamb [10], we take the linearized form of the NSWE (1) and search for solutions of the type

$$\eta^*(x^*,t^*) = Z(x^*)\cos\omega t^*, \quad u^*(x^*,t^*) = V(x^*)\sin\omega t^*. \tag{35}$$

By inserting (35) into (1) we obtain

$$h(x^*)\frac{d^2Z}{dx^{*2}} + \frac{dh(x^*)}{dx^*}\frac{dZ}{dx^*} + \frac{\omega^2 Z}{g} = 0, \tag{36}$$

$$V^* = -\frac{g}{\omega}\frac{dZ}{dx^*}. \tag{37}$$

Since the bathymetry is piecewise linear, at each segment $h_i(x^*) = -\alpha_i x^* + c_i$, where $\alpha_i = \tan\theta_i \neq 0$, c_i is a constant and the subscript i is indicative of the segment number from the shoreline to the seaward boundary. Then, (36) becomes a standard Bessel equation of order zero, and the general solution for Z_i and V_i is

$$Z_i(x^*) = A_i J_0(\sigma) + B_i Y_0(\sigma), \quad V_i(x^*) = \frac{2\omega}{\sigma\alpha_i}\frac{dZ_i}{d\sigma}, \tag{38}$$

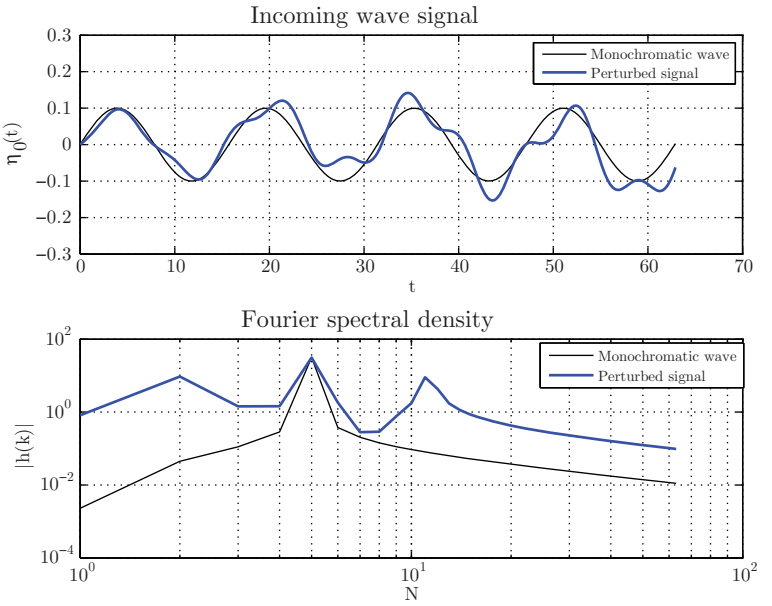

FIG. 9. Comparison of a typical monochromatic wave and a corresponding semi-randomly perturbed signal both in physical space (top) and Fourier space (bottom), where N is the Fourier mode and $h(k)$ is the spectral amplitude. Time t is in seconds, and the free-surface elevation $\eta_0(t)$ is in meters.

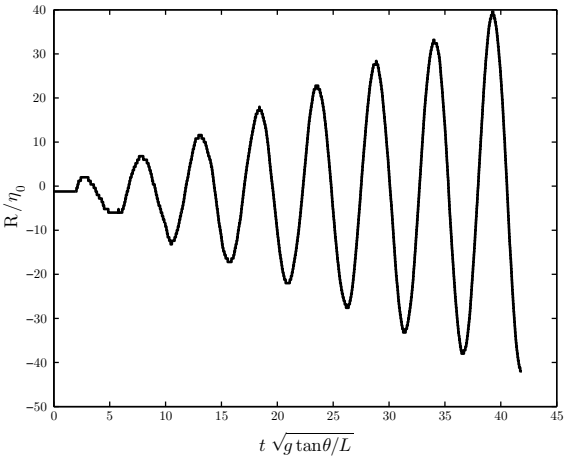

FIG. 10. Run-up timeseries of a perturbed resonant monochromatic wave when the slope is 0.02 and $L = 5000$ m.

where A_i and B_i are linear coefficients, J_n and Y_n are the nth order Bessel functions of the first and second kind respectively and

$$\sigma = \frac{2\omega}{\sqrt{g}}\sqrt{\frac{-x^* + \frac{c_i}{\alpha_i}}{\alpha_i}}. \tag{39}$$

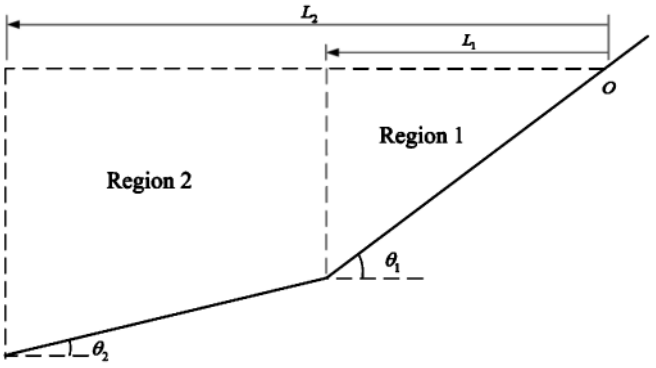

FIG. 11. Schematic of the piecewise linear bathymetry.

We now require continuity of the free surface elevation and of the horizontal fluxes at two adjacent segments and we prescribe a wave amplitude $Z_i = \eta_0 \cos \omega t^*$ at the seaward boundary. Here, for simplicity, we will focus on the case of two segments, but it can be generalized to an arbitrary number of segments as shown in [36]. In the first segment boundedness of the free surface elevation at the shoreline ($x^* = 0$) requires $B_1 = 0$. Since $J_0(0) = 1$, A_1 represents the run-up and therefore we will name it η_R. Hence, we have the following linear system of equations:

$$J_0(\sigma_1)\eta_R - J_0(\sigma_2)A_2 - Y_0(\sigma_2)B_2 = 0 \tag{40}$$

$$J_1(\sigma_1)\eta_R - J_1(\sigma_2)A_2 - Y_1(\sigma_2)B_2 = 0 \tag{41}$$

$$J_0(\sigma_3)A_2 + Y_0(\sigma_3)B_2 = \eta_0 \tag{42}$$

where

$$\sigma_1 = 2\omega\sqrt{\frac{L_1}{g\alpha_1}} \tag{43}$$

$$\sigma_2 = \frac{2\omega}{\alpha_2}\sqrt{\frac{\alpha_1 L_1}{g}} \tag{44}$$

$$\sigma_3 = \frac{2\omega}{\alpha_2}\sqrt{\frac{\alpha_2(L_2 - L_1) + \alpha_1 L_1}{g}}. \tag{45}$$

Then

$$\eta_R = \begin{vmatrix} 0 & -J_0(\sigma_2) & -Y_0(\sigma_2) \\ 0 & -J_1(\sigma_2) & -Y_1(\sigma_2) \\ \eta_0 & J_0(\sigma_3) & Y_0(\sigma_3) \end{vmatrix} \Big/ \begin{vmatrix} J_0(\sigma_1) & -J_0(\sigma_2) & -Y_0(\sigma_2) \\ J_1(\sigma_1) & -J_1(\sigma_2) & -Y_1(\sigma_2) \\ 0 & J_0(\sigma_3) & Y_0(\sigma_3) \end{vmatrix}. \tag{46}$$

Therefore, when the determinant in the denominator vanishes, the run-up becomes resonant (Figure 12). Furthermore, the shoreline velocity is now given by (38) as

$$V_s = \lim_{\sigma \to 0} -\frac{2\omega\eta_R}{\sigma\alpha_1} J_1(\sigma) \;\Rightarrow V_s = -\frac{\omega}{\alpha_1}\eta_R, \tag{47}$$

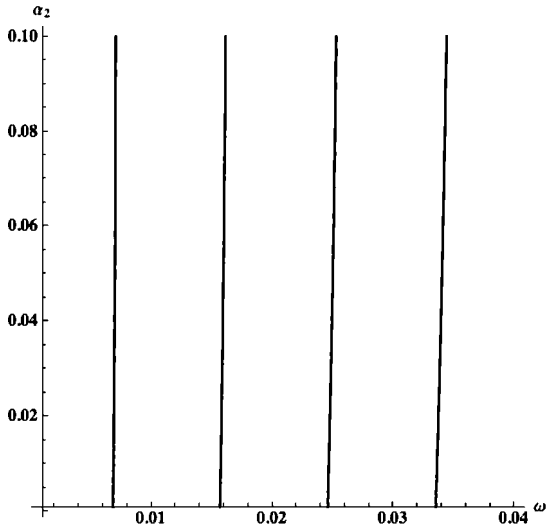

FIG. 12. Plot of the zeros of the determinant in the denominator of (46) as a function of ω and α_2 when $\alpha_1 = 0.02$, $L_1 = 5000$ m and $L_2 = 6000$ m.

which indicates that when the run-up is resonant, so is the shoreline velocity.[2] The same argument of course applies to the case of the infinite sloping beach (see Figure 4b). Numerical simulations performed in this setting with $\alpha_1 = 0.02$, $\alpha_2 = 0.01$, $L_1 = 5000$ m and $L_2 = 6000$ m ($\eta_0 = 0.1$ m) agree with the above analytical solution and again resonant wavelengths can be identified (Figure 13).

4.3. *Plane beach connected to a flat seafloor.* A more characteristic bathymetric profile consists of a constant depth region connected to a sloping beach, hereafter referred to as the canonical case (Figure 2). Using this profile, Madsen and Fuhrman [26] showed very good agreement between theory and their computations for a range of wavelengths $1 < \lambda_0/L < 7$ and wave nonlinearity $0.001 < \eta_0/h_0 < 0.01$, in which even a tsunami at $h_0 = 100$ m is fairly linear.[3] For their computations, they placed a relaxation zone close to the wave generation area so that no reflected waves from the beach interact with the forcing boundary, as there is no clear understanding of how to impose both incoming and outgoing waves at a boundary. It is convenient, because it allows for a reduction of the computational cost and has been used successfully in several other studies (e.g. [37], [38], [39]), but it is artificial. The length of the relaxation zone should be comparable to the wavelength, but the resonant wavelength is found to be greater than the beach length, which is why we could not employ it in the infinite slope case.

For the current bathymetric profile, our objectives were to investigate both whether resonance occurs and whether the existence of the relaxation zone plays any role on the run-up. Hence, we examined the run-up of monochromatic waves of amplitude $\eta_0 = 1.25$

[2]During run-up, the maximum shoreline velocity is not reached when the wave reaches its maximum run-up. So the joint resonance is not obvious. In fact at maximum run-up the velocity is zero.

[3]With $h_0 = 100$ m, the corresponding interval for η_0 is $0.1\text{m} < \eta_0 < 1\text{m}$.

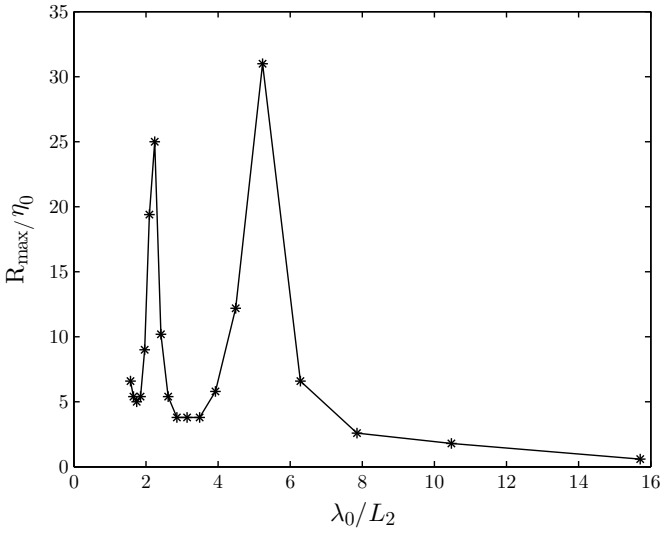

FIG. 13. Run-up amplification of monochromatic waves on a piecewise linear bathymetry consisting of two segments as a function of the nondimensional wavelength when $\alpha_1 = \tan\theta_1 = 0.02, \alpha_2 = \tan\theta_2 = 0.01, L_1 = 5000$ m and $L_2 = 6000$ m.

m on a plane beach with slope $\tan\theta = 0.02$, which reached a maximum depth $h_0 = 100$ m. We performed simulations with and without the relaxation zone. The setup without relaxation zone is more natural since no artificial filtering is used, but, at the same time, is more computationally demanding, due to the increased length of the constant depth region. In Figure 14, we observe that both with and without the relaxation zone, the computations predict slightly higher maximum run-up values than predicted by the theory in the nonbreaking regime, but the qualitative behavior is the same.

The discrepancies between theory and computations are higher when the use of a relaxation zone is avoided. Like Pelinovsky and Mazova [40], one can introduce the breaking number $Br = \omega^2\eta_R/g\alpha^2$. When $Br = 1$ or $\eta_R/\eta_0 = g\tan^2\theta/(\eta_0\omega^2)$, the analytical solution breaks down. When $Br > 1$, the wave breaks. According to Mei et al. [41], this criterion can only be used as a qualitative criterion. When waves are close to breaking, run-up amplification reaches its maximum. However, we cannot observe any significant resonance as we did in the infinite sloping beach example [2]. Wave breaking in the context of NSWE is demonstrated by the creation of a very steep wavefront, and actually it is a common practice in tsunami modeling, even when solving Boussinesq systems [42], to switch to NSWE as soon as the slope of the wavefront exceeds a threshold (e.g. [43, 44]). Above the breaking threshold, we observe in Figure 14 that theory and computations do not agree. However, the computations qualitatively follow the trend of the laboratory experiments presented by Ahrens [45], even though they refer to irregular wave run-up.

It is well known that in the context of NSWE, as waves propagate over a flat bottom, the wavefront tends to become steeper and the higher the wave nonlinearity, the faster

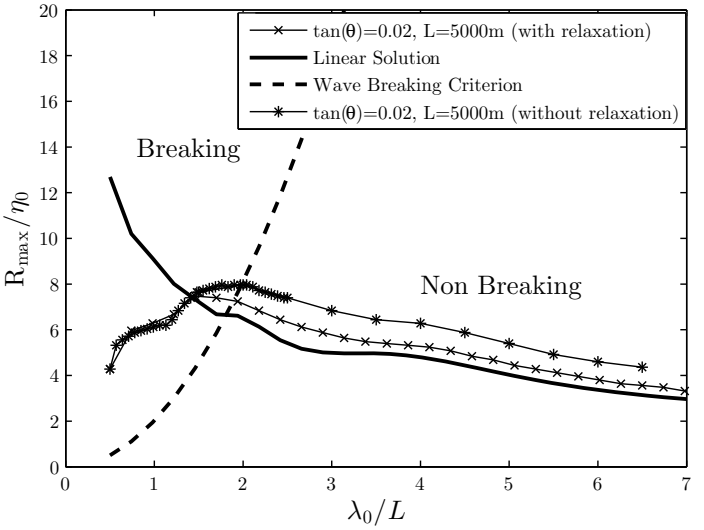

FIG. 14. Maximum run-up amplification as a function of nondimensional wavelength for the canonical case ($\eta_0 = 1.25$ m , $h_0 = 100$ m, $\tan\theta = 0.02$).

the wave steepening. Synolakis and Skjelbreia [46] have shown that while offshore and far from breaking, the wave evolves with Green's law and closer to breaking the evolution is more rapid, and they named it the Boussinesq regime. In the previous case, the discrepancies observed with and without the relaxation zone could be attributed to the different lengths of the constant bottom region (hereafter L_0). Before, the wave nonlinearity was $\eta_0/h = 0.0125$, and in order to increase the effect of wave steepening we doubled the incoming wave amplitude. Hence, we tested three different cases, namely the same two as before—one without a relaxation zone and $L_0 = 4\lambda_0$, one with a relaxation zone and $L_0 = 2\lambda_0$—and finally one with a relaxation zone, but now the constant depth region has a length equal to 4 wavelengths.

In Figure 15, we find L_0 is important, and hence the wavefront steepness is critical to run-up amplification. The existence of the relaxation zone does not affect the results when the constant depth region has a fixed length. The longer L_0, and therefore the wavefront steepness, the higher the run-up amplification, which in this case differs significantly from the theoretical curve (Figure 16), which is calculated for *symmetric* monochromatic waves.

In the previous cases, we only considered waves that were shorter than the distance from the undisturbed shoreline to the seaward boundary. However, in the piecewise linear bathymetry (Figure 11), we found that resonance is possible for wavelengths larger than this distance. The canonical case which we study in this section is a limiting example of the piecewise linear bathymetry as $\theta_i \to 0$, $i > 1$. Therefore, we performed simulations using a plane beach with slope $\tan\theta = 0.02$ connected to a region of constant depth ($h_0 = 100$ m), which has a length $L_0 = 3000$ m. This means that the distance from the initial shoreline to the seaward boundary is $L_t = 8000$ m. We used very small amplitude

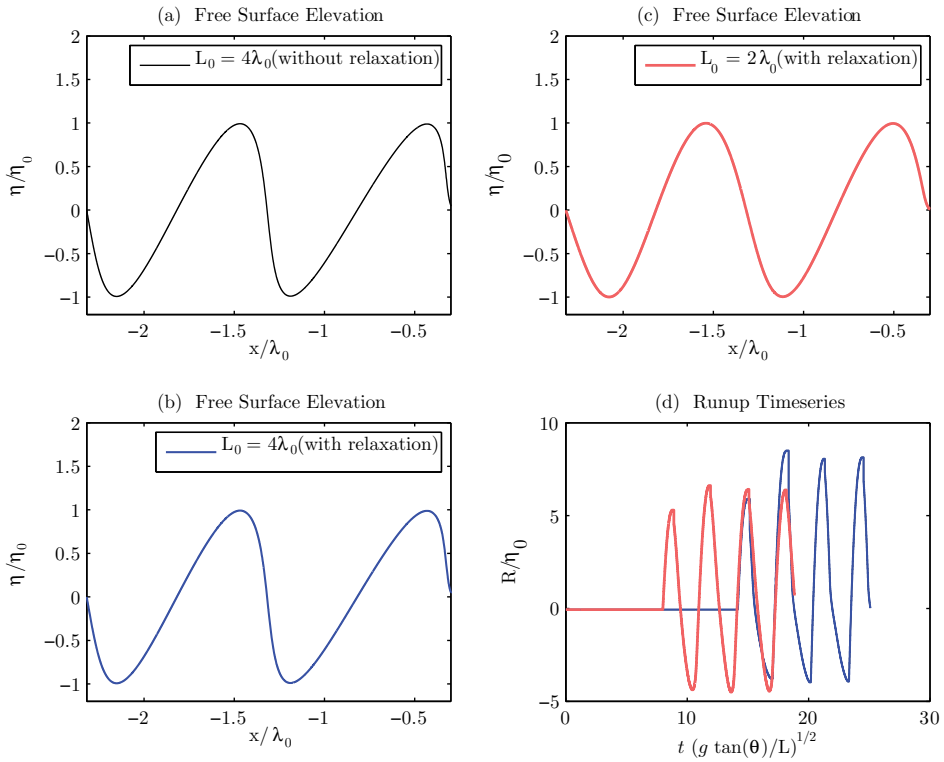

FIG. 15. Snapshots of free surface elevation over the constant depth region (a,b,c). The horizontal extent is two wavelengths offshore from the toe of the beach ($\lambda_0/L = 3.14$, $\eta_0 = 2.5$ m). Steeper wavefronts are observed when $L_0 = 4\lambda_0$. Run-up timeseries (d). Waves with steeper wavefront run-up higher.

waves ($\eta_0/h_0 = 0.001$) and we did not put a relaxation zone close to the generation region. For each simulation we sent four non-breaking waves. We observe in Figure 17 that resonance is possible for wavelengths larger than L_t and this result is closer to our observations from the piecewise linear bathymetry.

5. Discussion. Based on the findings of Stefanakis et al. [2], we reproduced their results of run-up amplification using milder, more geophysically relevant bottom slopes, and we showed that resonant run-up amplification on an infinite sloping beach is robust to modal perturbations.

Resonant run-up was confirmed by the laboratory experiments of Ezersky et al. [9] for monochromatic waves, and they also distinguished the resonant run-up frequencies from the natural frequencies of the system. The first resonant regime ($\lambda_0/L = 5.2$, where λ_0 is the incoming wavelength and L is the horizontal beach length) was achieved for nonbreaking waves as in [9]. Moreover, we note that our findings present similarities to those of Bruun and Johannesson [47] or Bruun and Günbak [18], who described a resonance phenomenon of short wave run-up on sloping structures. They described it

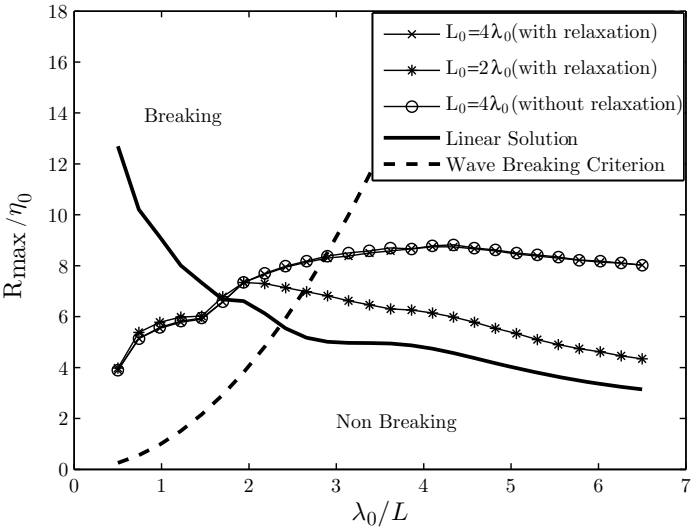

FIG. 16. Maximum run-up amplification as a function of nondimensional wavelength for the canonical case ($\eta_0 = 2.5$ m, $h_0 = 100$ m, $\tan\theta = 0.02$).

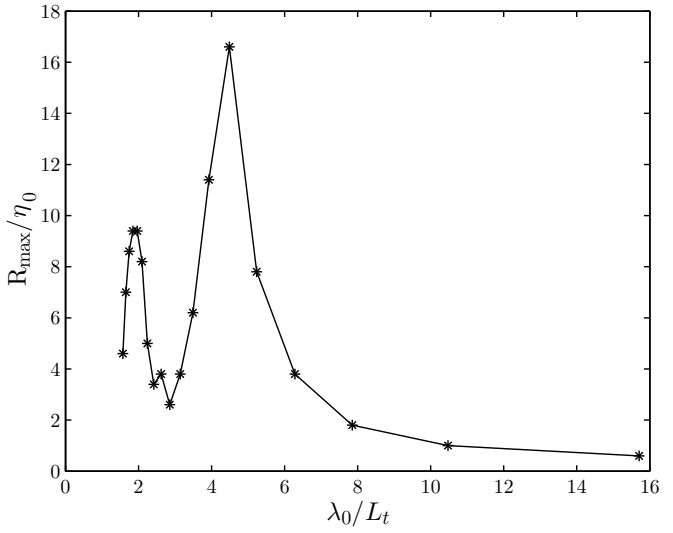

FIG. 17. Maximum run-up amplification as a function of nondimensional wavelength for the canonical case when $L_t = 8000$ m is the distance from the undisturbed shoreline to the seaward boundary ($\eta_0 = 0.1$ m, $h_0 = 100$ m, $\tan\theta = 0.02$).

as wave breaking taking place at the point of maximum run-down simultaneously with the arrival of the subsequent wave. Here, we do not see wave breaking, but there is a synchronization between the maximum run-down of a wave and the arrival of the next wave (Figure 6).

Run-up resonance in the laboratory experiments of Ezersky et al. [9] was achieved for breaking waves as well, but for these cases they did not comment on the location where the breaking takes place. Hence, probably wave breaking is not the key factor to the resonant mechanism. Long wave breaking in the context of NSWE and its physical demonstration is a subtle issue. As noted by Synolakis [21], the NSWE tend to predict wave breaking sooner than it actually happens in nature.

The same resonant mechanism is found when the bathymetry is piecewise linear. However, when the beach is connected to a constant depth region, the phenomenology is different. No resonant regimes are observed when the incoming wavelength is smaller than the distance between the initial shoreline and the seaward boundary. The maximum run-up amplification is found close to the breaking limit for nearly symmetric low amplitude waves. In that case the linear theory is in close agreement with the results for non-breaking waves. Nevertheless, the steepness of the wavefront plays an important role on run-up, with increasing steepness leading to higher run-up. It is not clear, though, if it is the wavefront steepness which is responsible for the increase of run-up values or the wave asymmetry (skewness). Increasing the incoming wavelength more than the wave propagation distance to the undisturbed shoreline results in observing resonant regimes similar to those found in the piecewise linear bathymetry example, which can be thought of as the limiting case when the angles $\theta_i \to 0\,,\ i > 1$.[4] It is of interest to report that Keller and Keller [19] tried to reproduce numerically their analytical solution and found a peak which corresponds to the resonant frequency in our simulations. However, they dismissed these results by saying that their computational scheme was not good enough. We can assert that in linear theory, the existence or not of resonance depends on the geometry the bathymetry has at the seaward boundary.

The discrepancies of the results using the two bathymetric profiles raise questions about the role boundary conditions play both physically and numerically, and more importantly about the character of the flow (stationary vs. transient).

Acknowledgements. This work was funded by EDSP of ENS-Cachan, the Cultural Service of the French Embassy in Dublin (first author), the China Scholarship Council (second author), the ERC under the research project ERC-2011-AdG 290562-MULTIWAVE, SFI under the programme ERC Starter Grant - Top Up, Grant 12/ERC/E2227 and the Strategic and Major Initiatives scheme of University College Dublin.

References

[1] G. F. Carrier and H. P. Greenspan, *Water waves of finite amplitude on a sloping beach*, J. Fluid Mech. **4** (1958), 97–109. MR0096462 (20 #2945)

[2] T. S. Stefanakis, F. Dias, and D. Dutykh, *Local run-up amplification by resonant wave interactions*, Phys. Rev. Lett., 107:124502, 2011.

[3] A. B. Rabinovich, I. Vilibic, and S. Tinti, *Meteorological tsunamis: Atmospherically induced destructive ocean waves in the tsunami frequency band*, Phys. Chem. Earth, 34:891 – 893, 2009.

[4] Even though the length of the computational domain is not a physical parameter, it is of importance from an operational point of view when one wants to predict run-up elevation based on recorded wave signals at an offshore location. In that case, the incoming wavelength can be either larger or smaller than the beach length.

[4] Costas E. Synolakis and Eddie N. Bernard, *Tsunami science before and beyond Boxing Day 2004*, Philos. Trans. R. Soc. Lond. Ser. A Math. Phys. Eng. Sci. **364** (2006), no. 1845, 2231–2265, DOI 10.1098/rsta.2006.1824. MR2244672 (2007b:86013)

[5] Y. Tsuji, F. Imamura, H. Matsutomi, C. Synolakis, P. Nanang, Jumadi, S. Harada, S. Han, K. Arai, and B. Cook, *Field survey of the East Java earthquake and tsunami of June 3, 1994*, Pure Appl. Geophys., 144:839–854, 1995.

[6] H. M. Fritz, W. Kongko, A. Moore, B. McAdoo, J. Goff, C. Harbitz, B. Uslu, N. Kalligeris, D. Suteja, K. Kalsum, V. V. Titov, A. Gusman, H. Latief, E. Santoso, S. Sujoko, D. Djulkarnaen, H. Sunendar, and C. Synolakis, *Extreme runup from the 17 July 2006 Java tsunami*, Geophys. Res. Lett., 34:L12602, 2007.

[7] H. Fritz, C. Petroff, P. Catalán, R. Cienfuegos, P. Winckler, N. Kalligeris, R. Weiss, S. Barrientos, G. Meneses, C. Valderas-Bermejo, C. Ebeling, A. Papadopoulos, M. Contreras, R. Almar, J. Dominguez, and C. Synolakis, *Field survey of the 27 February 2010 Chile tsunami*, Pure Appl. Geophys., 168:1989–2010, 2011.

[8] S. T. Grilli, J. C. Harris, T. S. Bakhsh, T. L. Masterlark, C. Kyriakopoulos, J. T. Kirby, and F. Shi, *Numerical simulation of the 2011 Tohoku tsunami based on a new transient FEM co-seismic source: Comparison to far- and near-field observations*, Pure Appl. Geophys., 170(6–8) 1333–1359, 2013.

[9] A. Ezersky, N. Abcha, and E. Pelinovsky, *Physical simulation of resonant wave run-up on a beach*, Nonlinear Proc. Geoph., 20(1):35–40, 2013.

[10] Horace Lamb, *Hydrodynamics*, 6th ed., with a foreword by R. A. Caflisch [Russel E. Caflisch]. Reprint of the 1932 sixth ed., Cambridge Mathematical Library, Cambridge University Press, Cambridge, 1993. MR1317348 (96f:76001)

[11] J. W. Miles, *Resonant response of harbours: an equivalent-circuit analysis*, J. Fluid Mech., 46:241–265, 1971.

[12] K. Kajiura. Local behaviour of tsunamis. In D. Provis and R. Radok, editors, *Waves on water of variable depth*, volume 64 of *Lecture Notes in Physics*, pages 72–79. Springer Berlin / Heidelberg, 1977. MR0475212 (57 #14830)

[13] Yehuda Agnon and Chiang C. Mei, *Trapping and resonance of long shelf waves due to groups of short waves*, J. Fluid Mech. **195** (1988), 201–221, DOI 10.1017/S0022112088002381. MR985437 (90m:76021)

[14] Géraldine L. Grataloup and Chiang C. Mei, *Localization of harmonics generated in nonlinear shallow water waves*, Phys. Rev. E (3) **68** (2003), no. 2, 026314, 9, DOI 10.1103/PhysRevE.68.026314. MR2010086 (2004h:76022)

[15] W. Munk, F. Snodgrass, and F. Gilbert, *Long waves on the continental shelf: an experiment to separate trapped and leaky modes*, J. Fluid Mech., 20:529–554, 1964.

[16] A. B. Rabinovich and A. S. Leviant, *Influence of seiche oscillations on the formation of the long-wave spectrum near the coast of the Southern Kuriles*, Oceanology, 32:17–23, 1992.

[17] U. Kânoğlu, V. Titov, B. Aydın, C. Moore, T. S. Stefanakis, H. Zhou, M. Spillane, and C. Synolakis, *Focusing of long waves with finite crest over constant depth*, Proc. R. Soc. A, 469(2153), 2013.

[18] P. Bruun and A. R. Günbak, *Stability of sloping structures in relation to* $\xi = tan\alpha/\sqrt{H/L_0}$ *risk criteria in design*, Coast. Eng., 1:287 – 322, 1977.

[19] J. B. Keller and H. B. Keller, *Water wave run-up on a beach*, Technical report, Department of the Navy, Washington, DC, 1964.

[20] George F. Carrier, *Gravity waves on water of variable depth*, J. Fluid Mech. **24** (1966), 641–659. MR0200009 (33 #8149)

[21] C. Synolakis, *The runup of solitary waves*, J. Fluid Mech., 185:523–545, 1987.

[22] S. Tadepalli and C. Synolakis, *The run-up of N-waves on sloping beaches*, Proc. R. Soc. Lond. A, 445:99–112, 1994.

[23] M. Brocchini and D. H. Peregrine, *Integral flow properties of the swash zone and averaging*, J. Fluid Mech, 317:241–273, 1996.

[24] U. Kânoğlu and C. Synolakis, *Initial value problem solution of nonlinear shallow water-wave equations*, Phys. Rev. Lett., 97:148501, 2006.

[25] Matteo Antuono and Maurizio Brocchini, *The boundary value problem for the nonlinear shallow water equations*, Stud. Appl. Math. **119** (2007), no. 1, 73–93, DOI 10.1111/j.1365-2966.2007.00378.x. MR2324442 (2008e:76014)

[26] P. A. Madsen and D. R. Fuhrman, *Run-up of tsunamis and long waves in terms of surf-similarity*, Coastal Engineering, 55:209 – 223, 2008.

[27] P. A. Madsen, D. R. Fuhrman, and H. A. Schaffer, *On the solitary wave paradigm for tsunamis*, J. Geophys. Res., 113(C12), 2008.
[28] George F. Carrier, Tai Tei Wu, and Harry Yeh, *Tsunami run-up and draw-down on a plane beach*, J. Fluid Mech. **475** (2003), 79–99, DOI 10.1017/S0022112002002653. MR2012495 (2004h:86002)
[29] S. Tadepalli and C. E. Synolakis, *Model for the leading waves of tsunamis*, Phys. Rev. Lett., 77:2141–2144, 1996.
[30] Costas Emmanuel Synolakis, *On the roots of* $f(z) = J_0(z) - iJ_1(z)$, Quart. Appl. Math. **46** (1988), no. 1, 105–107. MR934685 (89d:33013)
[31] J. Billingham and A. C. King, *Wave motion*, Cambridge Texts in Applied Mathematics, Cambridge University Press, Cambridge, 2000. MR1811404 (2001k:35001)
[32] Jean-Michel Ghidaglia and Frédéric Pascal, *The normal flux method at the boundary for multidimensional finite volume approximations in CFD*, Eur. J. Mech. B Fluids **24** (2005), no. 1, 1–17, DOI 10.1016/j.euromechflu.2004.05.003. MR2102914 (2005m:76121)
[33] Denys Dutykh, Theodoros Katsaounis, and Dimitrios Mitsotakis, *Finite volume schemes for dispersive wave propagation and runup*, J. Comput. Phys. **230** (2011), no. 8, 3035–3061, DOI 10.1016/j.jcp.2011.01.003. MR2774329 (2012g:65168)
[34] Denys Dutykh, Raphaël Poncet, and Frédéric Dias, *The VOLNA code for the numerical modeling of tsunami waves: generation, propagation and inundation*, Eur. J. Mech. B Fluids **30** (2011), no. 6, 598–615. MR2906226
[35] C. Synolakis, E. Bernard, V. Titov, U. Kanoglu, and F. Gonzalez, *Standards, criteria, and procedures for NOAA evaluation of tsunami numerical models*, Technical report, NOAA/Pacific Marine Environmental Laboratory, 2007.
[36] Utku Kânoğlu and Costas Emmanuel Synolakis, *Long wave runup on piecewise linear topographies*, J. Fluid Mech. **374** (1998), 1–28, DOI 10.1017/S0022112098002468. MR1660967 (99g:86001)
[37] S. Mayer, A. Garapon, and L. S. Soerensen, *A fractional step method for unsteady free-surface flow with applications to non-linear wave dynamics*, Int. J. Num. Meth. Fl., 28:293–315, 1998.
[38] P. A. Madsen, H. B. Bingham, and Hua Liu, *A new Boussinesq method for fully nonlinear waves from shallow to deep water*, J. Fluid Mech. **462** (2002), 1–30, DOI 10.1017/S0022112002008467. MR1919980 (2003d:76023)
[39] Y. Lu, H. Liu, W. Wu, and J. Zhang, *Numerical simulation of two-dimensional overtopping against seawalls armored with artificial units in regular waves*, J. Hydrodyn. Ser. B, 19(3):322 – 329, 2007.
[40] E. N. Pelinovsky and R. K. Mazova, *Exact analytical solutions of nonlinear problems of tsunami wave run-up on slopes with different profiles*, Nat. Hazards, 6:227–249, 1992.
[41] C. C. Mei, M. Stiassnie, and D. Yue, *Theory and applications of ocean surface waves*, In *Advanced Series on Ocean Engineering, vol. 23*, World Scientific, Singapore, 2005.
[42] M. Kazolea, A. I. Delis, I. K. Nikolos, and C. E. Synolakis, *An unstructured finite volume numerical scheme for extended 2D Boussinesq-type equations*, Coastal Engineering, 69:42–66, 2012.
[43] F. Shi, J. T. Kirby, J. C. Harris, J. D. Geiman, and S. T. Grilli, *A high-order adaptive time-stepping TVD solver for Boussinesq modeling of breaking waves and coastal inundation*, Ocean Modelling, 43-44:36 – 51, 2012.
[44] M. Tissier, P. Bonneton, F. Marche, F. Chazel, and D. Lannes, *A new approach to handle wave breaking in fully non-linear Boussinesq models*, Coastal Engineering, 67:54–66, 2012.
[45] J. P. Ahrens, *Irregular wave runup on smooth slope*, CETA No. 81-17. U.S. Army Corps of Engineers, Coastal Engineering Research Center, FT. Belvoir, VA, 1981.
[46] C. Synolakis and J. Skjelbreia, *Evolution of maximum amplitude of solitary waves on plane beaches*, J. Waterw. Harbors Port Coastal Ocean Eng., 119(3):323–342, 1993.
[47] P. Bruun and P. Johannesson,*A critical review of the hydraulics of rubble mound structures*, Technical report, The Norwegian Institute of Technology, Trondheim, 1974.